MOLECULAR PHARMACOLOGY, 26:1-9

Two Affinity States of R_i Adenosine Receptors in Brain Membranes

Analysis of Guanine Nucleotide and Temperature Effects on Radioligand Binding

MARTIN J. LOHSE, VOLKER LENSCHOW, AND ULRICH SCHWABE

Pharmakologisches Institut der Universität Heidelberg, 6900 Heidelberg, Federal Republic of Germany

Received November 14, 1983; Accepted April 6, 1984

SUMMARY

The binding of agonists and antagonists to R_i adenosine receptors of synaptosomal membranes from rat and bovine brain was studied. The effects of guanine nucleotides and temperature were analyzed with the aid of computerized curve fitting. Evidence is presented for two different states of the receptor: one of high and one of low affinity for agonists. Antagonists bind to both states with the same affinity. The two states are characterized by saturation, competition, and kinetic experiments with very similar results. Guanine nucleotides cause transition of the high- to the low-affinity state. The ratio of the K_D values for the two affinity states is 90–150 in rat brain but only 10 in bovine brain. The proportions of the two affinity states are the same for all agonists tested; in the absence of exogenous guanine nucleotides, 75% of the total receptor population is in the high-affinity state, whereas in the presence of guanine nucleotides only 5% remain in the high-affinity state. Binding of antagonists to the receptor is enthalpy-driven whereas binding of the agonist (−)-N^6-phenylisopropyladenosine to the high-affinity state of the receptor is entropy-driven. Binding of the agonist to the low-affinity state is enthalpy-driven and thus similar to the binding of antagonists. Our data indicate that guanine nucleotides convert the R_i adenosine receptor from a high- to a low-agonist affinity state and that agonist binding shows thermodynamic differences from antagonist binding only when it is to the high-affinity state of the receptor.

INTRODUCTION

The original observation by Sattin and Rall (1) of adenosine-induced cyclic AMP formation in brain suggested that specific receptors for this nucleoside might be linked to adenylate cyclase. Subsequently, adenosine receptors that mediate either stimulation or inhibition of cyclic AMP were identified by adenylate cyclase studies. On the basis of different potencies of adenosine analogues, they have been classified as inhibitory R_i or A_1 and stimulatory R_a or A_2 adenosine receptors (2, 3). Both types of adenosine receptors can be found in rat brain (4–6).

Adenosine influences a great number of physiological processes; in the central nervous system it inhibits neurotransmitter release and neuronal firing and may function as a neuromodulator (7); these effects seem to be mediated via R_i adenosine receptors (8). Recently, radioligand binding of adenosine agonists and antagonists to adenosine receptors in brain has been demonstrated (9–11). The high-affinity binding and the appropriate structure-activity profiles suggest that these radioligands bind to R_i adenosine receptors. It has further been shown that the binding of several adenosine agonists is decreased by guanine nucleotides (9, 12, 13), but the exact nature of this effect has not been fully elucidated. In order to clarify the mechanism of interaction with the R_i adenosine receptor in brain, we have compared the effect of guanine nucleotides and temperature on the binding of agonists and antagonists. We have used computer-based methods of curve fitting for quantitative analysis of the binding data. From the data presented it is concluded that the R_i adenosine receptor in rat brain can exist in two affinity states for agonists which have different thermodynamic characteristics.

EXPERIMENTAL PROCEDURES

Materials

[^{3}H]PIA[1] (specific activity 49.9 Ci/mmole) and [^{3}H]DPX (specific activity 13.4 Ci/mmole) were obtained from New England Nuclear

This work was supported by a grant from the Deutsche Forschungsgemeinschaft (Schw. 83/13-1). The costs of publication of this article were defrayed in part by the payment of page charges. This article must therefore be hereby marked "*advertisement*" in accordance with 18 U.S.C. Section 1734 solely to indicate this fact.

[1] The abbreviations used are: [^{3}H]PIA, (−)-N^6-phenylisopropyl [^{3}H] adenosine; [^{3}H]DPX, 1,3-diethyl-8-[^{3}H]phenylxanthine; Gpp(NH)p, 5′-guanylylimidodiphosphate; IBMX, 3-isobutyl-1-methylxanthine; (−)-PIA, (−)-N^6-phenylisopropyladenosine; CHA, N^6-cyclohexyladenosine.

0026-895X/84/040001-09$02.00/0

Corporation (Dreieich, Federal Republic of Germany). Adenosine deaminase from calf intestine (200 units/mg), GTP, GMP, and Gpp(NH)p were obtained from Boehringer Mannheim (Mannheim, Federal Republic of Germany). IBMX, theophylline, and 2-chloroadenosine were from Sigma Chemical Company (München-Taufkirchen, Federal Republic of Germany). (−)-PIA and CHA were kindly provided by Dr. K. Stegmeier, Boehringer Mannheim. All other chemicals were of analytical or best commercially available grade from standard sources.

Methods

Preparation of brain synaptosomal membranes. Synaptosomal membranes from rat and bovine brain were prepared according to the method described by Whittaker (14). Male Sprague-Dawley rats (150–250 g) were killed by cervical dislocation, and the forebrains were quickly removed and immediately placed in 0.32 M sucrose (4°). Bovine cerebral cortex was obtained from a local slaughterhouse and was placed into 0.32 M sucrose within 30 min of slaughter. The tissue was homogenized in a glass-Teflon homogenizer in 10 volumes of sucrose (clearing 0.2 mm, at 500 rpm for 30 sec). The homogenate was centrifuged at 1,000 × *g* for 10 min to remove the nuclear fraction, and the supernatant was centrifuged at 10,000 × *g* for 10 min to give the P_2 fraction. The pellets were resuspended in 0.32 M sucrose with a Polytron homogenizer (setting 6, 10 sec) and layered on top of a discontinuous sucrose gradient consisting of 10 ml of 1.2 M and 10 ml of 0.8 M sucrose. After centrifugation at 53,000 × *g* for 150 min in a swing-out rotor, the B-fraction containing mainly synaptosomes was collected at the 1.2 M/0.8 M interface. It was diluted with an equal volume of water and centrifuged for 60 min at 100,000 × *g*. The pellets were resuspended in 10 ml of water and left on ice for 30 min to give synaptosomal membranes. After a final centrifugation step at 48,000 × *g* for 10 min, the membranes were resuspended in water in a concentration of 6–10 mg of protein per milliliter, frozen in liquid nitrogen, and stored at −18° until assayed for binding. Protein was measured according to the method of Lowry *et al.* (15).

Binding assay. Measurement of [^{3}H]PIA binding to synaptosomal membranes was carried out as described previously (10). Membranes were diluted in 50 mM Tris-HCl buffer (pH 7.4) to a protein concentration of 1 mg/ml and incubated for 30 min at 37° with adenosine deaminase (0.2 unit/ml) to remove endogenous adenosine. The preincubation resulted in no change in equilibrium studies as compared with addition of adenosine deaminase at the start of incubation but was necessary for kinetic studies with short incubation times. In order to enable a comparison of different experiments, the preincubation procedure was the same for all experiments. Binding of [^{3}H]PIA to membranes (100 μg of protein per tube) was carried out in 50 mM Tris-HCl buffer (pH 7.4) in a total volume of 1 ml; [^{3}H]PIA was present in a final concentration of 1 nM. Other substances were added as indicated. Incubation was carried out at 37° for 45 min and was terminated by filtration of a 900-μl aliquot through a Whatman GF/B filter. Filters were immediately washed twice with 5 ml of Tris-HCl buffer (0°); after addition of 10 ml of scintillation fluid, samples were allowed to equilibrate for 12 hr before counting in a liquid scintillation counter with an efficiency of approximately 50%.

Binding of [^{3}H]DPX was carried out in essentially the same way, except that the final volume was reduced to 250 μl and the labeled ligand was present in a final concentration of 10 nM for rat brain and 1 nM for bovine brain; only 3 ml of buffer were used to wash the filter each of two times. Incubation time was in general 15 min. In experiments at different incubation temperatures, the incubation time was 30 min; this was sufficient to reach equilibrium at all temperatures.

Nonspecific binding was determined in the presence of 10 μM (−)-PIA in the case of [^{3}H]PIA binding and of 1 mM theophylline in the case of [^{3}H]DPX binding. It amounted to about 5% and 25%, respectively. The same amount of nonspecific binding was obtained with 1 mM theophylline in the case of [^{3}H]PIA binding or 10 μM (−)-PIA in the case of [^{3}H]DPX binding. Nonspecific binding was not subtracted for data analysis of competition curves.

In some experiments, separation of bound and free [^{3}H]PIA was achieved by a centrifugation technique. At the end of the incubation period, tubes were centrifuged at 12,000 × *g* for 3 min. The supernatant was aspirated and the pellet rinsed with 500 μl of incubation buffer, which was immediately aspirated. The tips of the tubes were cut off, 10 ml of scintillation fluid were added, and the samples were counted as described above. Nonspecific binding, as defined by the addition of 10 μM (−)-PIA or 1 mM theophylline, was about 20% of total binding.

Data were analyzed by the computer modeling method described by De Lean *et al.* (16), which allows independent analysis of various parameters as well as a comparison of different models. Significance of improvement of a fit was tested as described below. Parameters estimated in this study were K_i or K_D values, B_{max} values, and nonspecific binding; if two states of high and low affinity were present, values given are K_H and K_L; R_H and R_L denote the percentage of the respective states calculated from the estimated B_{max} values. It should be noted that if the radioligand itself has different affinities for the two states, the amount of radioligand actually bound to each state may substantially differ from the respective R_H and R_L values. Slope factors were calculated from indirect Hill plots ("pseudo" Hill coefficients).

Kinetic data were fitted by nonlinear regression using the following equations.:

$$\text{Dissociation: } B(t) = \sum_j B_j \cdot e^{-k_j t}$$

$$\text{Association: } B(t) = \sum_j B_j \cdot (1 - e^{-(k_{+j} \cdot L_T + k_{-j})t})$$

where B denotes the total ligand bound, B_j is the ligand bound at equilibrium to the receptor R_j, k_{-j} is the dissociation constant, and k_{+j} the association constant for the receptor R_j; L_T is the total concentration of ligand. To simplify the integration for the association, pseudo-first order conditions were assumed, i.e, that the concentration of the radioligand was much higher than that of the receptor. This was acceptable since in our experiments the bound ligand never exceeded 5% of the total ligand; however, analysis of the dissociation curve was more exact, as no such simplification was needed. B_j can be expressed as a function of the variables k_{+j} and k_{-j}; at equilibrium $d(B)/dt = 0$ and hence $k_{+j}(L)(R_j) = k_{-j}(B_j)$, which is under pseudo-first order conditions ($L_T \gg B$): $k_{+j}(L_T)(R_{Tj} - B_j) = k_{-j}(B_j)$, where R_{Tj} is the total concentration of receptor R_j, which can be solved to give

$$B_j = \frac{k_{+j}(L_T)(R_{Tj})}{k_{+j}(L_T) + k_{-j}}$$

The data were fitted by use of a computer-modeling method described by Provencher (17), using the general equation $y = \sum_j \alpha_j e^{-\lambda_j t}$, and the kinetic constants were calculated from the respective α and λ values.

The fit was tested for $j = 1, 2, 3$, and the improvement was tested by an F-test. A model was judged to be appropriate when the fit was significantly ($p < 0.001$) better than the preceding one and not significantly worse ($p > 0.001$) than the model assuming $j + 1$ sites. Parameters were shared to a common value if this did not significantly worsen the fit. In general, the simplest model was considered to be appropriate. Using these criteria, in no case more than two receptor states had to be assumed.

Thermodynamic parameters were calculated from van't Hoff plots as described by Weiland *et al.* (18), using the following equations: (a) $\Delta G° = -R \cdot T \cdot \ln K_A$, (b) $\Delta H° = -a \cdot R$, and (c) $\Delta S° = (\Delta H° - \Delta G°)/T$, where $\Delta G°$ (kcal/mole) is the Gibbs' free-energy change, $\Delta H°$ (kcal/mole) the enthalpy change, and $\Delta S°$ (cal/mole·deg) the entropy change; a is the slope of the van't Hoff plot.

RESULTS

Guanine nucleotides inhibited [^{3}H]PIA binding in a concentration-dependent manner; GTP, GDP, and the hydrolysis-resistant GTP analogue Gpp(NH)p were

about equally effective in reducing binding of [^{3}H]PIA, with IC_{50} values of 0.5 μM, 0.5 μM, and 0.9 μM, respectively. GMP had effects only at concentrations 100-fold higher than those required by the other guanine nucleotides, and the other nucleotide triphosphates (ATP, ITP) were ineffective. Maximally effective concentrations of the guanine nucleotides caused a decrease in [^{3}H]PIA binding to less than 10% of the initial values. The binding was not further decreased by the use of concentrations of GTP above 100 μM. Binding of [^{3}H]DPX was not inhibited by guanine nucleotides.

In order to elucidate the mechanism of action of guanine nucleotides, saturation experiments were carried out in the absence or presence of 100 μM GTP. The specific binding of both radioligands was saturable. The addition of GTP (100 μM) did not affect binding of [^{3}H]DPX (Fig. 1). The Scatchard plots were linear in the absence and in the presence of GTP, suggesting a homogeneous population of binding sites, and the K_D and B_{max} values were almost identical (control, 68.2 nM and 1.22 pmoles/mg of protein; with GTP, 69.2 nM and 1.26 pmoles/mg of protein). Similar K_i values were obtained in competition experiments (data not shown).

In the case of [^{3}H]PIA binding, however, the addition of GTP caused marked changes in the saturation isotherm (Fig. 2). In the absence of GTP the isotherm conformed to a simple hyperbola. The Scatchard plot was linear, with a K_D of 1.4 nM and a B_{max} of 0.74 pmole/mg of protein. In the presence of GTP the saturation isotherm was biphasic and saturation was achieved only at relatively high concentrations of [^{3}H]PIA. The Scatchard plot gave a hyperbola, indicating the presence of two affinity states. One had a B_{max} of 0.09 pmole/mg of protein and a K_D of 2.1 nM; the other had a B_{max} of 0.97 pmole/mg of protein and a K_D of 161 nM. The K_D of the high-affinity state was in good agreement with the K_D determined in the absence of GTP.

Because of the relatively high K_L, the saturation experiment in the presence of GTP was repeated using a centrifugation technique. This revealed a higher B_{max} of the low-affinity state but resulted in no significant change in the other parameters (K_H 2.2 nM, K_L 158 nM,

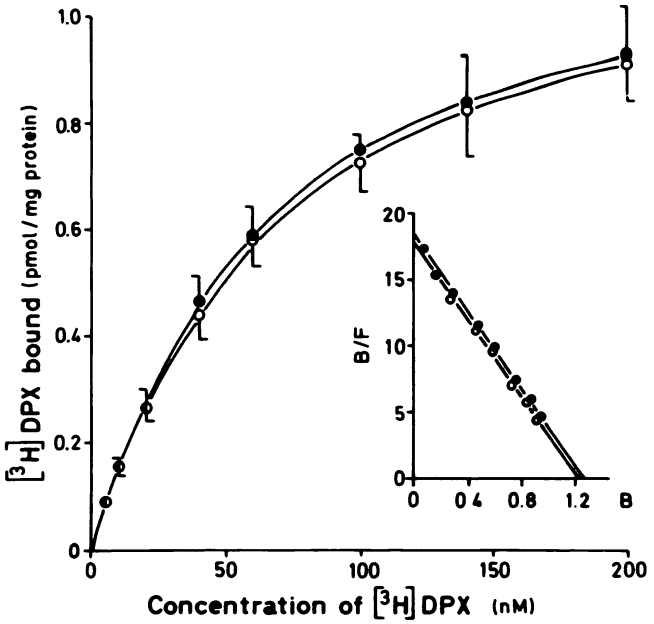

FIG. 1. *Saturation of [^{3}H]DPX binding to rat brain synaptosomal membranes*

Specific binding of [^{3}H]DPX in the absence (○) and in the presence (●) of 100 μM GTP was determined at 37° as described under Methods. Values are the means ± standard error of the mean of three separate experiments performed in duplicate. In the *inset*, the Scatchard plot of the same data is shown. K_D and B_{max} values were 68.2 nM and 1.22 pmoles/mg of protein in the absence of GTP and 69.2 nM and 1.26 pmoles/mg of protein in the presence of GTP.

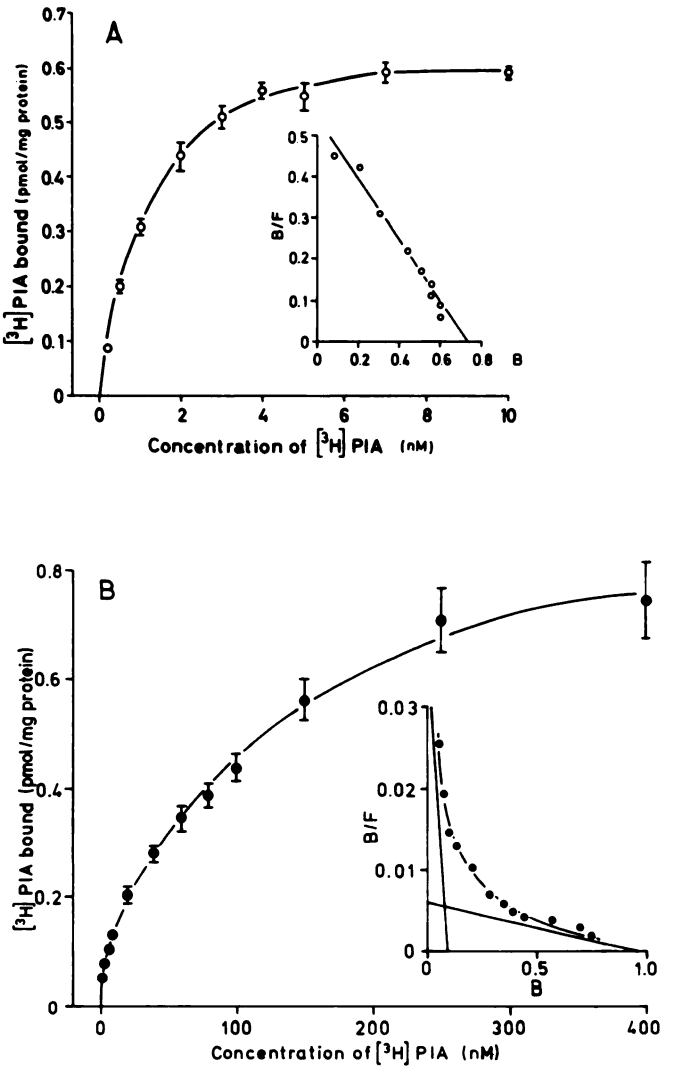

FIG. 2. *Saturation of [^{3}H]PIA binding to rat brain synaptosomal membranes*

Specific binding of [^{3}H]PIA in the absence (A) and in the presence (B) of 100 μM GTP was determined as described under Methods. Values are the means ± standard error of the mean of three separate experiments performed in duplicate. In the *inset*, the Scatchard plots of the same data are shown. In the absence of GTP (A) the plot is linear, giving a K_D of 1.4 nM and a B_{max} of 0.74 pmole/mg of protein. In the presence of GTP (B), two states are present and the values are as follows: high-affinity state K_H 2.1 nM, B_{max_H} 0.09 pmole/mg of protein; low-affinity state K_L 161 nM, B_{max_L} 0.97 pmole/mg of protein. The proportions of the two affinity states are R_H 8% and R_L 92%.

B_{max_H} 0.08 pmole/mg of protein and B_{max_L} 1.34 pmoles/mg of protein). Use of the filtration technique thus results in a 25% loss of low-affinity binding but gives the same estimate for the affinity of the low-affinity state.

In the presence of 4 mM $MgCl_2$, Gpp(NH)p and GTP have been reported to induce an increase in the B_{max} for [^{3}H]DPX and a state of medium affinity for the agonist [^{3}H]CHA as assessed by saturation experiments (19). Therefore, the saturation experiments were repeated in the presence of 4 mM $MgCl_2$. This did not change the saturation isotherm of [^{3}H]DPX binding; 100 μM GTP had no effect on either the K_D (65.9 nM versus 64.2 nM without GTP) or the B_{max} (1.22 pmoles/mg of protein versus 1.24 pmoles/mg of protein without GTP). In the case of [^{3}H]PIA binding, Mg^{2+} induced a higher proportion of receptors in the high-affinity state but did not alter the K_D values (K_H 2.4 nM, K_L 148 nM, B_{max_H} 0.22 pmole/mg of protein and B_{max_L} 0.93 pmole/mg of protein).

Kinetic studies were undertaken in order to confirm the results of the saturation studies with [^{3}H]PIA. Association and dissociation of [^{3}H]PIA binding were measured in the absence and presence of 100 μM GTP (Fig. 3). In the absence of GTP, both curves were monophasic, giving a kinetic K_D of 1.9 nM. In the presence of GTP, the dissociation and also the association were biphasic. Analysis of the dissociation curve gave a kinetic K_H of 1.2 nM and K_L of 137 nM; analysis of the association curve (which is the less correct analysis since we assumed pseudo-first order conditions) gave similar results. These values are in good agreement with those from saturation studies.

In addition, the kinetic experiments showed a constant equilibrium in both the absence and presence of GTP for more than 2 hr, demonstrating the stability of high- and low-affinity binding.

Competition for [^{3}H]PIA as well as [^{3}H]DPX binding was determined for several drugs known to interact with R_i adenosine receptors (Figs. 4 and 5). GTP decreased the potency of agonists in competition experiments with both the radiolabeled agonist and antagonist, whereas the potency of antagonists was not altered by GTP. If [^{3}H]PIA was used as the labeled ligand, the competition with (−)-PIA gave a sigmoidal competition curve with a slope factor of 0.96 and a K_i of 2.4 nM (Fig. 4). In the presence of GTP the competition curve was shifted to the right, as indicated by an increase in the IC_{50} from 3.0 to 12.1 nM. In addition, the curve now exhibited a slope factor of 0.63. Computer analysis indicated the presence of two affinity states; K_i values were 1.2 nM and 135 nM, and the proportions of the two sites were R_H 3% and R_L 97%. These results agree well with those obtained from saturation experiments.

Competition for [^{3}H]PIA binding by the antagonist IBMX (Fig. 4) was monophasic in the absence of GTP, indicating a single affinity state for both the agonist

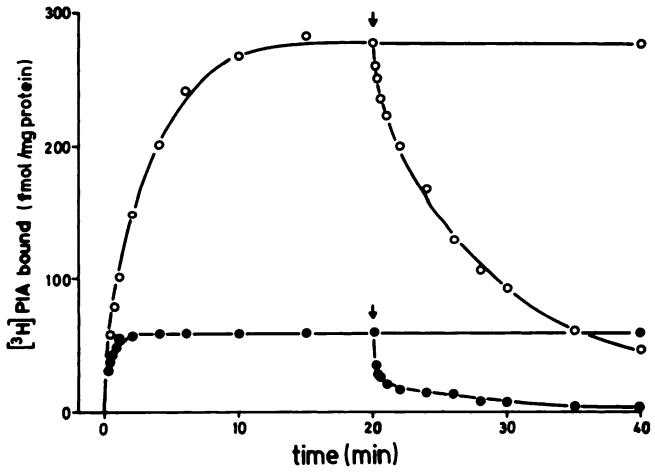

FIG. 3. *Kinetics of [^{3}H]PIA binding to rat brain synaptosomal membranes*

Association and dissociation of [^{3}H]PIA were determined in the absence (○) and in the presence (●) of 100 μM GTP. The association was started by addition of the membrane preparation. After 20 min, the dissociation was started by addition of (−)-PIA (10 μM, *arrow*). Filtration was carried out at individual time points. The radioligand concentration was 1 nM in the absence and 4 nM in the presence of GTP. All other conditions were as described under Methods. Values are the means of three separate experiments performed in duplicate. The curves were analyzed by nonlinear regression as described under Methods.

In the absence of GTP, the curves were monophasic, with k_{+1} = 0.053 nM^{-1} min^{-1} and k_{-1} = 0.102 min^{-1} (K_D = 1.9 nM). In the presence of GTP, the curves were biphasic. Analysis of the dissociation curve gave k_{+H} = 0.082 nM^{-1} min^{-1}, k_{+L} = 0.039 nM^{-1} min^{-1}, k_{-H} = 0.12 min^{-1} and k_{-L} = 5.24 min^{-1} (K_H = 1.2 nM, K_L = 137 nM); analysis of the association curve gave similar values (K_H 1.9 nM; K_L 121 nM).

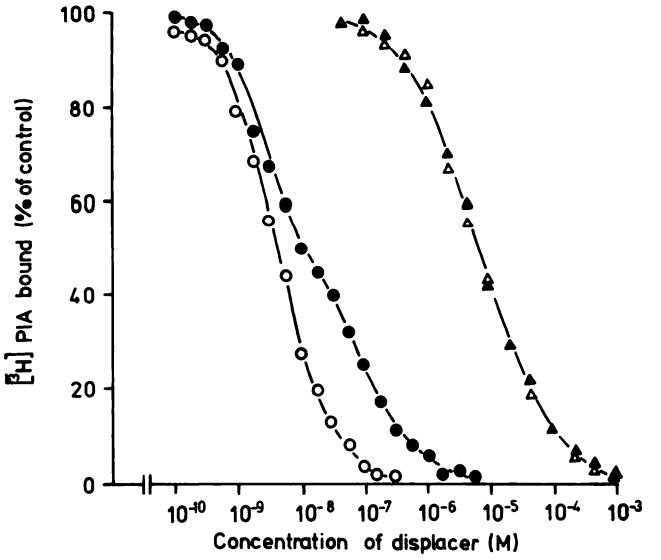

FIG. 4. *Competition for [^{3}H]PIA binding to rat brain synaptosomal membranes by (−)-PIA and IBMX*

Specific binding of [^{3}H]PIA in the absence (*open symbols*) and presence (*closed symbols*) of 100 μM GTP was determined at various concentrations of (−)-PIA (○, ●) and IBMX (△, ▲). Control binding (100%) was 231 fmoles/mg of protein in the absence of GTP and 33 fmoles/mg of protein in the presence of GTP. Analysis of the curves as described under Methods gave the following estimates: (−)-PIA without GTP, K_H 2.4 nM, R_H 100%; with GTP, K_H 1.2 nM, K_L 135 nM, R_H 4% and R_L 96%. IBMX had the same affinity for both states, with K_i 4.1 μM (without GTP) and 4.6 μM (with GTP); in the presence of GTP, R_H was estimated at 5% and R_L at 95%. The discrepancy between the radioligand actually bound to the two affinity states and the corresponding R values should be noted (see Methods). Separation of bound and free radioligand was achieved by centrifugation.

TABLE 1

Binding parameters for competition for [^{3}H]DPX binding by adenosine agonists and antagonists

Rat brain synaptosomal membranes were incubated with 10 nM [^{3}H]DPX at 37° for 15 min as described under Methods. Displacement of [^{3}H]DPX binding was determined by using at least eight concentrations of the displacing compound in the presence and absence of 100 μM GTP. For each experiment with the various compounds, estimates of the high (K_H) and low (K_L) affinity dissociation constants, the maximal number of binding sites (B_{max}), the percentage of total receptors in the high-affinity state (%R_H), the slope factor calculated as the Hill coefficient (n_H), and the ratio K_L/K_H as a measure for the GTP-induced shift in affinity are given. For K_H, K_L, and K_L/K_H, geometric means are shown with 95% confidence limits in parentheses. All other results are expressed as means ± standard error of the mean of five experiments.

Compound	B_{max}	R_H	K_H	K_L	GTP shift	Slope factor
	fmoles/mg	%	*nM*	*nM*	K_L *(GTP)/*K_H	
(−)-PIA	950 ± 30	72	1.3 (1.1–2.4)	194 (62–611)		0.51 ± 0.01
(−)-PIA + GTP[a]	1,160 ± 40	—		200 (160–251)	149 (80–227)	0.87 ± 0.02
CHA	930 ± 20	74	2.6 (2.0–3.5)	224 (158–317)		0.49 ± 0.01
CHA + GTP[a]	1,050 ± 50	—		244 (157–380)	93 (57–151)	0.91 ± 0.07
NECA	960 ± 30	72	8.2 (6.2–10.9)	503 (234–1,082)		0.50 ± 0.01
NECA + GTP[a]	1,130 ± 20	—		1,179 (989–1,404)	143 (121–170)	0.87 ± 0.02
2-Chloroadenosine	1,040 ± 20	74	14.4 (7.9–26.1)	1,205 (209–6,932)		0.49 ± 0.02
2-Chloroadenosine + GTP[a]	1,180 ± 20	—		1,476 (761–2,864)	103 (35–298)	0.82 ± 0.03
Theophylline[b]	1,120 ± 60	—		11,000 (8,600–14,000)		0.88 ± 0.01
Theophylline + GTP	1,230 ± 60	—		11,000 (9,700–12,500)	1.0[c] (0.9–1.1)	0.90 ± 0.05
IBMX[b]	1,020 ± 70	—		3,170 (2,610–3,860)		0.92 ± 0.04
IBMX + GTP	1,170 ± 80	—		2,400 (2,090–2,750)	0.8[c] (0.7–0.9)	0.97 ± 0.02

[a] Models to one state, all in low-affinity form (R_L 100%).
[b] Models to one state of homogeneous affinity ($K_H = K_L$); K_i values are given under K_L.
[c] K_i (GTP)/K_i (control).

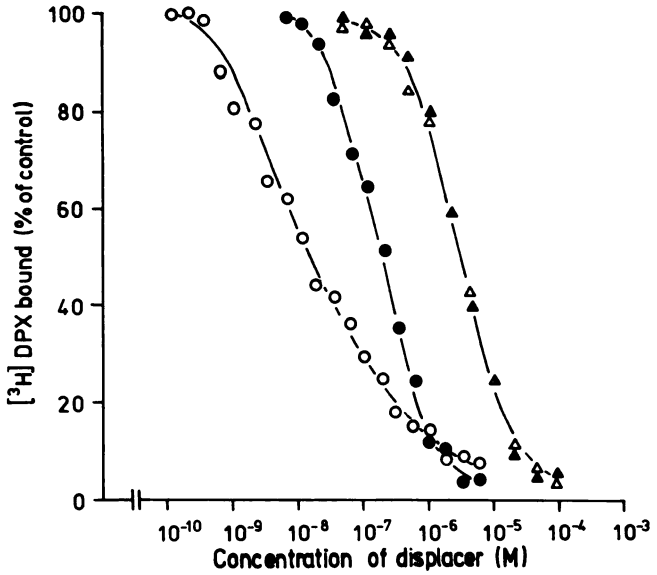

FIG. 5. *Competition for [^{3}H]DPX binding to rat brain synaptosomal membranes by (−)-PIA and IBMX*

Specific binding of [^{3}H]DPX in the absence (*open symbols*) and presence (*closed symbols*) of 100 μM GTP was determined at different concentrations of (−)-PIA (○, ●) and IBMX (△, ▲). Control binding (100%) was 130 fmoles/mg of protein in the absence of GTP and 142 fmoles/mg of protein in the presence of GTP. Analysis of the curves as described under Methods gave the following estimates: (−)-PIA without GTP, K_H 2.2 nM, K_L 192 nM, R_H 69% and R_L 31%; in the presence of GTP, only one affinity state could be detected with K_L 155 nM (R_L 100%). With IBMX, only one state of homogeneous affinity was seen with K_i 2.7 μM (without GTP) and 2.3 μM (with GTP); R_H and R_L could not be determined.

radioligand and the antagonist competitor. In the presence of GTP, two affinity states for [^{3}H]PIA have to be assumed, with R_H 5% and R_L 95%. The affinity of IBMX was the same for both states, and the K_i values of IBMX obtained in the presence (4.6 μM) and absence of GTP (4.1 μM) were not significantly different.

If [^{3}H]DPX was used as the labeled ligand, the competition curve of agonists was shallow with a slope factor of about 0.5 (Fig. 5). The addition of GTP steepened the curve and the slope factor approached unity. At the same time, GTP caused a very marked shift of the IC_{50} to higher concentrations. Computer analysis of the curves showed the presence of two affinity states in the absence of GTP. The K_i values for (−)-PIA were 2.2 nM and 192 nM, respectively, and the proportions of states of high and low affinity for the agonist were R_H 69% and R_L 31%. In the presence of GTP, only one affinity state could be detected with a slope factor near unity (n_H = 0.98). The K_i value was 155 nM, which is close to the value of the low-affinity state in the absence of GTP. Finally, competition for [^{3}H]DPX binding by the antagonist IBMX was studied (Fig. 5). The curves in both the presence and absence of GTP were monophasic, and the K_i values obtained were not significantly different. Both compounds seemed to have the same affinity for the high- and low-agonist affinity state, and thus R_H and R_L cannot be determined.

Values for several agonists and antagonists at the R_i receptor are given in Table 1. GTP caused a 90- to 150-fold shift in the K_i of all agonists investigated, but did not alter the affinity of the antagonists. The K_i of ago-

nists in the presence of GTP was in general reasonably close to the K_i of the low-affinity state in the absence of GTP. It should be noted, however, that the K_i of the low-affinity state was difficult to determine accurately in the absence of GTP, as the proportion was only 20%. Therefore, the ratio of the K_i of the low- and high-affinity state was calculated as the shift induced by the presence of GTP [K_L(+GTP)/K_H(control)].

In bovine brain GTP has been reported to cause less pronounced shifts in the IC_{50} of agonists in competing for [^{3}H]DPX (12). Therefore, we examined the effects of 100 μM GTP on inhibition of [^{3}H]DPX binding by (−)-PIA in bovine cerebral cortex in order to look for species differences (Fig. 6). When these results were compared with those obtained in rat brain, two basic differences could be observed: in the absence of GTP only a high-affinity state was found with a K_H of 0.6 nM, whereas in the presence of GTP the high- and the low-affinity state were seen with K_H 0.4 nM and K_L 8.3 nM. Only about 80% of the receptor population was in the low-affinity state in the presence of GTP, and the ratio K_L/K_H was about 14 as compared with the factor of about 150 in rat brain.

Binding reactions have been reported to be temperature-dependent phenomena. In particular, agonist and antagonist binding has been shown to differ in its thermodynamic characteristics (18). Therefore, we examined the effects of temperature on the high- and low-affinity states of the R_i receptor. In preliminary studies we verified that (a) equilibrium of [^{3}H]DPX binding was attained after a 30-min incubation time at all temperatures used and (b) the effects of temperature on the radioligand [^{3}H]DPX and the displacer for nonspecific binding, theophylline, were about equal, resulting in a 4-fold increase in the affinity at 0° as compared with 37° (data not shown). Therefore, 1 mM theophylline could be used at all temperatures to define nonspecific binding.

Figure 7 shows that the competition curve of (−)-PIA in the absence of GTP was shifted to higher concentrations at 0° as compared with 37°. On the other hand, in the presence of GTP the curve was shifted to lower concentrations at lower temperatures. This results in a substantial decrease in the net effect of GTP at 0°.

These effects were studied in more detail by measuring the competition for [^{3}H]DPX binding by theophylline and (−)-PIA at various temperatures; K_i values for theophylline and the K_H and K_L values as well as R_H and R_L for (−)-PIA were calculated as before. The van't Hoff plot of the data (Fig. 8; Table 2) revealed striking dissimilarities between the high- and the low-affinity states. At high temperatures, (−)-PIA was more potent at the high-affinity state but less potent at the low-affinity state; theophylline—as well as other antagonists (data not shown)—was less potent at higher temperatures. Binding of the antagonist as well as of the agonist to the low-affinity state seemed to be enthalpy-driven with small increases in the entropy. On the other hand, binding of the agonist to the high-affinity state was associated with an increase in the enthalpy and was entropy-driven. In addition, the proportion of receptor in the high-affinity state in the absence of GTP was only about 30–40% at 0° as compared with 70–85% at higher temperatures.

DISCUSSION

In several receptor systems GTP decreases the affinity of agonists (20); in addition, in some receptor systems [for example, the dopamine receptor in the pituitary (21)], the affinity of antagonists is also altered by GTP, but in a reciprocal way.

Our study shows that in the case of the R_i adenosine receptor, GTP reduces the affinity of agonists by a factor of 90–150 in rat brain and of 10 in bovine brain, but does

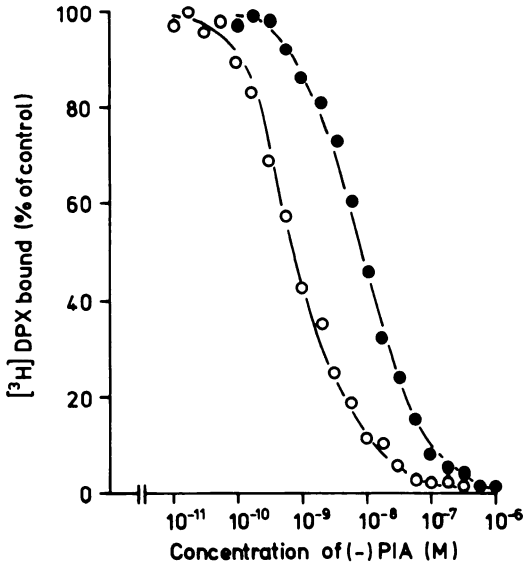

FIG. 6. *Competition for [^{3}H]DPX binding by (−)-PIA in bovine cerebral cortex*

Specific binding of [^{3}H]DPX in the absence (○) and presence (●) of 100 μM GTP was determined at different concentrations of (−)-PIA. Control binding (100%) was 360 fmoles/mg of protein. Analysis of the curves gave the following estimates: without GTP, only one affinity state was detected with K_H 0.6 nM and R_H 100%; with GTP, K_H 0.4 nM, K_L 8.3 nM, R_H 14% and R_L 86%.

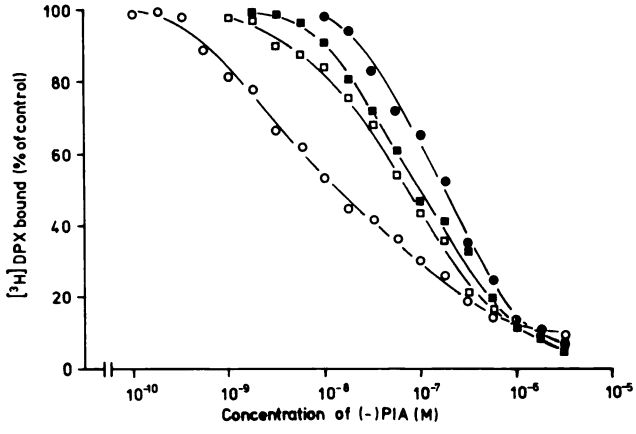

FIG. 7. *Competition for [^{3}H]DPX binding to rat brain synaptosomal membranes by (−)-PIA at 37° and 0°*

Specific binding of [^{3}H]DPX in the absence (*open symbols*) and presence of 100 μM GTP (*closed symbols*) was determined at different concentrations of (−)-PIA at 37° (○, ●) and 0° (□, ■). Data for 37° are taken from Fig. 5. At 0°, 100% represents 203 fmoles/mg of protein. The following estimates were obtained for 0°: without GTP, K_H 7.7 nM, K_L 74.1 nM, R_H 27%, and R_L 73%; with GTP, K_L 62.5 nM and R_L 100%.

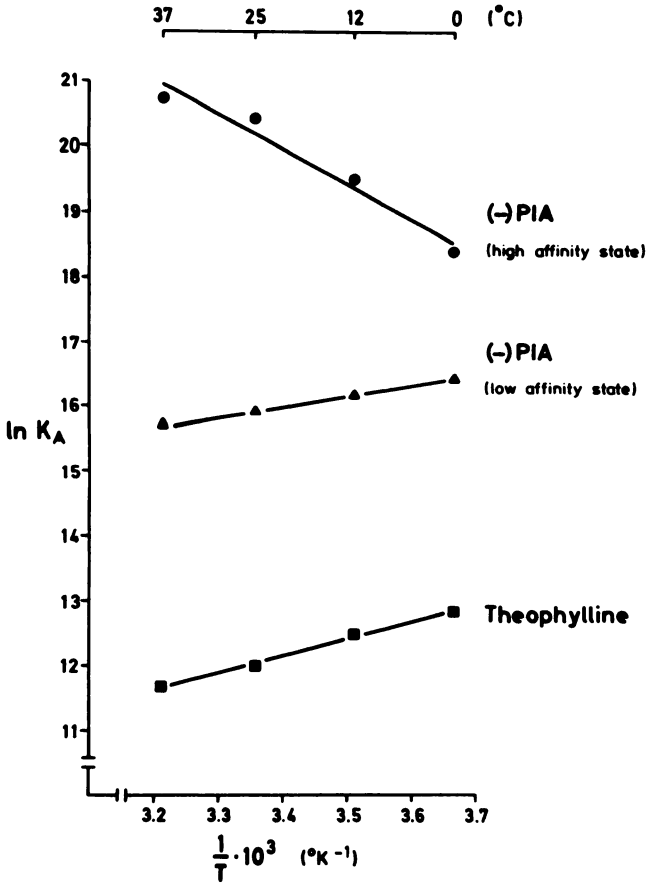

FIG. 8. *Van't Hoff plots for theophylline and (−)-PIA binding to R_i adenosine receptors of rat brain*

Competition experiments using 10 nM [^{3}H]DPX were carried out at various temperatures as described under Methods. K_D values for [^{3}H]DPX were obtained from saturation studies, and competition curves were analyzed as described under Methods. Binding of (−)-PIA to the high- and low-affinity states was measured in the absence and presence of 100 μM GTP, and the K_H and K_L were calculated as in Table 1. K_i values for theophylline were determined in the absence of GTP. K_A values are $1/K_i$ or $1/K_H$, $1/K_L$, respectively. Values are the means of three separate experiments performed in duplicate at each temperature. Correlation coefficients are $r = 0.99$ (theophylline), $r = 1.00$ [(−)-PIA, low-affinity state], and $r = -0.97$ [(−)-PIA, high-affinity state]. In the presence of GTP, only the low-affinity state was observed; in the absence of GTP, R_H was 73% at 37°, 84% at 25°, 79% at 12°, and 43% at 0°.

not influence the binding of antagonists. The differences between bovine and rat brain may reflect true species differences but might also be due to the time lag between slaughter and tissue preparation in the case of bovine brain. These results agree with the data reported by Goodman *et al.* (12), but contrast with those of Yeung and Green (19), who found a marked increase in the B_{max} for [^{3}H]DPX in the presence of GTP and 4 mM $MgCl_2$. However, we found no significant change in either B_{max} or K_D (K_i) values in saturation and competition experiments when GTP was added in the presence and in the absence of Mg^{2+}, although in some experiments a minor increase in [^{3}H]DPX binding was observed in the presence of GTP; an increase of about 8% has also been reported by Bruns *et al.* (9). The inhibition of [^{3}H]PIA binding by GTP seems to be due to a transition from a high- to a low-agonist affinity state. There is good agreement in the K_H and the K_L values obtained from saturation, kinetic, and competition experiments in the absence and in the presence of GTP. This suggests that the low-affinity state in the absence of GTP—as seen in the displacement of [^{3}H]DPX by (−)-PIA—is identical with the state induced by GTP. It may be due to residual GTP in the membrane preparation.

TABLE 2

Thermodynamic parameters of binding to rat brain R_i adenosine receptors

K_i values were obtained by computer modeling of competition curves against [^{3}H]DPX at 0°, 12°, 25° and 37°. The changes in free energy ($\Delta G°$), enthalpy ($\Delta H°$), and entropy ($\Delta S°$) of binding at 37° were calculated as described under Methods.

	$\Delta G°$	$\Delta H°$	$\Delta S°$
	kcal/mole	*kcal/mole*	*cal/mole deg*
(−)-PIA (high-affinity state)	−12.7	10.8	76
(−)-PIA (low-affinity state)	−9.7	−3.4	20
Theophylline	−7.2	−5.3	6.2

In the absence of GTP, about 30% of the receptor population is in the low-affinity state. This is not observed when [^{3}H]PIA is used as the radioligand in low concentrations, which explains the lower B_{max} obtained from saturation with [^{3}H]PIA in the absence of GTP as compared with [^{3}H]DPX. In the presence of GTP, 95% of the receptor population is in the low-affinity state. This high proportion can be detected in studies with [^{3}H]PIA in spite of the high K_L value and is seen in saturation as well as in competition experiments. The small percentage of receptors in the high-affinity state ($R_H = 5\%$) is too small to be detected by computer analysis of competition experiments using [^{3}H]DPX as the radioligand and an agonist as the displacer (Fig. 5; Table 1), although the Hill coefficients are not quite at unity. [^{3}H]PIA dissociates rapidly from receptors in the low-affinity state; this explains lower B_{max} obtained from saturation experiments with [^{3}H]PIA in the presence of GTP as compared with that seen with [^{3}H]DPX, when the filtration technique is used. Using the centrifugation technique, the B_{max} values are the same. This supports the notion that both [^{3}H]DPX and [^{3}H]PIA label the same receptor population in rat brain (R_i) and that in this species [^{3}H]DPX does not label R_a receptors (22).

In addition to these two agonist affinity states Yeung and Green (19) have described a state of medium affinity for agonists which they see in saturation experiments with [^{3}H]CHA in the presence of Gpp(NH)p; in the same experiment they observed a marked reduction in the B_{max}. The most likely explanation for this discrepancy is the limited concentration range of the radioligand used by these authors (10–100 nM), which is beyond the K_H (1.8 nM) and below the K_L (430 nM) reported. The use of Gpp(NH)p instead of GTP does not seem to be of importance in this respect, as similar results were observed with both nucleotides. Another difference is the presence of 4 mM $MgCl_2$ in the incubation buffer of the study cited above; however, we also observed a curvilinear Scatchard plot in the presence of GTP and Mg^{2+} when a wide range

of radioligand concentrations was employed. Divalent cations have been demonstrated to reduce the effects of GTP on agonist binding to R_i adenosine receptors (12); our results demonstrate that this is due to a higher proportion of receptors in the high-affinity state when both GTP and Mg^{2+} are present as compared with GTP alone. Therefore, we have omitted Mg^{2+} in all other experiments in order to demonstrate the effects of GTP more clearly. In agreement with our results are those published by Goodman *et al.* (12), who reported no change in the B_{max}, and K_H and K_L values of 0.5 and 5 nM for [^{3}H]CHA in bovine brain in the absence and in the presence of GTP. This ratio of K_L/K_H agrees very well with the ratio seen in our experiments with bovine brain. In addition, these authors found linear Scatchard plots under both conditions, suggesting a 100% transition to the low-affinity state in the presence of GTP.

The proportions of high- and low-affinity states as well as the ratio K_L/K_H estimated from competition for [^{3}H] DPX binding are about the same for all agonists tested. Similar results have been reported for the dopamine receptor of the porcine anterior pituitary (21). In the case of the *beta*-adrenergic receptor from frog erythrocytes, different proportions have been described for full and partial agonists, and there was a good correlation of intrinsic activity and the ratio K_L/K_H (23). As no partial agonists for the R_i adenosine receptor are known, it cannot be said whether or not these are receptor differences.

Binding of ligands to their receptors has been shown to be a temperature-dependent process, and agonists and antagonists can be distinguished by their different thermodynamic characteristics (18). In the case of the adrenergic *beta*-receptor, the dopamine receptor, and the muscarinic receptor, binding of agonists is mainly enthalpy-driven and binding of antagonists is entropy-driven (24–26). Similarly, agonist binding to *alpha*$_2$-adrenergic receptors appears to be favored at lower temperatures (27). On the other hand, opiate agonists have lower affinities at low temperatures (28), indicating that binding of these agonists to their receptor is entropy-driven. The binding of agonists to the R_i adenosine receptor is also entropy-driven (22), and binding of antagonists is enthalpy-driven. These differences indicate that interaction of an agonist with a receptor linked to adenylate cyclase may be associated both with an increase or a decrease of standard enthalpy and entropy, depending on the nature of the receptor. Although agonist binding causes interaction with a GTP regulatory protein in most if not all of these receptor systems, the thermodynamic parameters of this process seem to be governed by more complex events. Different interactions with other membrane constituents as well as the surrounding fluids may be responsible for the differences observed (18).

No analysis of thermodynamic characteristics has so far been reported for the different agonist affinity states of a receptor. Our data suggest that there are fundamental differences between the binding of agonists to the low- and to the high-affinity state of the R_i receptor. Whereas binding to the high-affinity state is clearly different from antagonist binding, binding to the low affinity state closely resembles that of antagonists. Thus, binding of the agonist to the low-affinity states is largely enthalpy-driven with an additional entropy component which also characterizes binding of antagonists.

It is thought that coupling of a receptor with the GTP-regulatory protein induces the high-affinity state (12, 29). This is confirmed by successful curve fitting assuming a ternary complex model (30). Binding of GTP to this complex may (a) activate adenylate cyclase and (b) cause disaggregation of the complex and thus induce the low-affinity state. This theory can also serve to explain the different thermodynamic characteristics of the high- and low-affinity state: the differences between agonists and antagonists may be due to their different capability to induce coupling to the GTP regulatory protein. If no such coupling can be induced by agonists because of the presence of GTP, the agonist behaves thermodynamically like the antagonist. Thus, the thermodynamic characteristics of ligand binding to the R_i adenosine receptor seem to be determined not only by the nature of the ligand but also by the state of the receptor-GTP regulatory protein complex.

ACKNOWLEDGMENTS

We should like to thank Drs. T. Mansky and C. Kleinschmidt, Max-Planck-Institut für Biophysikalische Chemie, Göttingen, for their help in the computerized fitting of the kinetic data. The technical assistance of Ms. U. Schwaab and Ms. I. Hermann is gratefully acknowledged.

REFERENCES

1. Sattin, A., and T. W. Rall. The effect of adenosine and adenine nucleotides on the cyclic adenosine 3′-5′-phosphate content of guinea pig cerebral cortex slices. *Mol. Pharmacol.* **6**:13–23 (1970).
2. Van Calker, D., M. Müller, and B. Hamprecht. Adenosine inhibits the accumulation of cyclic AMP in cultured brain cells. *Nature (Lond.)* **276**:839–841 (1978).
3. Londos, C., D. M. F. Cooper, and J. Wolff. Subclasses of external adenosine receptors. *Proc. Natl. Acad. Sci. U. S. A.* **77**:2551–2554 (1980).
4. Prémont, J., M. Perez, and J. Bockaert. Adenosine-sensitive adenylate cyclase in rat striatal homogenates and its relationship to dopamine- and Ca^{2+}-sensitive adenylate cyclases. *Mol. Pharmacol.* **13**:662–670 (1977).
5. Cooper, D. M. F., C. Londos, and M. Rodbell. Adenosine receptor-mediated inhibition of rat cerebral cortical adenylate cyclase by a GTP-dependent process. *Mol. Pharmacol.* **18**:598–601 (1980).
6. Ebersolt, C., J. Prémont, and J. Bockaert. Inhibition of brain adenylate cyclase by A_1 adenosine receptors: pharmacological characteristics and locations. *Brain Res* **267**:123–129 (1983).
7. Phillis, J. W., and P. H. Wu. The role of adenosine and its nucleotides in central synaptic transmission. *Prog. Neurobiol.* **16**:187–239 (1981).
8. Schubert, P., K. Lee, M. Reddington, and G. Kreutzberg. Synaptic modulation by adenosine: electrophysiological and biochemical characteristics, in *Regulatory Function of Adenosine* (R. M. Berne, T. W. Rall, and R. Rubio eds.). Martinus Nijhoff Publishers, The Hague, Boston and London, 439–454 (1983).
9. Bruns, R. F., J. W. Daly, and S. H. Snyder. Adenosine receptors in brain membranes: binding of N^6-cyclohexyl[^{3}H]adenosine and 1,3-diethyl-8-[^{3}H] phenylxanthine. *Proc. Natl. Acad. Sci. U. S. A.* **77**:5547–5551 (1980).
10. Schwabe, U., and T. Trost. Characterization of adenosine receptors in rat brain by (−)[^{3}H]N^6-phenylisopropyladenosine. *Naunyn-Schmiedeberg's Arch. Pharmacol.* **313**:179–187 (1980).
11. Williams, M., and E. A. Risley. Biochemical characterization of putative central purinergic receptors by using 2-chloro[^{3}H]adenosine, a stable analog of adenosine. *Proc. Natl. Acad. Sci. U. S. A.* **77**:6892–6896 (1980).
12. Goodman, R. R., M. J. Cooper, M. Gavish, and S. H. Snyder. Guanine nucleotide and cation regulation of the binding of [^{3}H]cyclohexyladenosine and [^{3}H]diethylphenylxanthine to adenosine A_1 receptors in brain membranes. *Mol. Pharmacol.* **21**:329–335 (1982).
13. Gavish, M., R. R. Goodman, and S. H. Snyder. Solubilized adenosine receptors in the brain: regulation by guanine nucleotides. *Science (Wash. D. C.)* **215**:1633–1635 (1980).
14. Whittaker, V. P. The synaptosome, in *Handbook of Neurochemistry* (A. Lajtha, ed.), Vol. 2. Plenum Press, New York, 327–364 (1969).

15. Lowry, O. H., N. J. Rosebrough, A. L. Farr, and R. J. Randall. Protein measurement with the Folin phenol reagent. *J. Biol. Chem.* **193**:265–275 (1951).
16. De Lean, A., A. A. Hancock, and R. J. Lefkowitz. Validation and statistical analysis of a computer modeling method for quantitative analysis of radioligand binding data for mixtures of pharmacological receptor subtypes. *Mol. Pharmacol.* **21**:5–16 (1982).
17. Provencher, S. W. An eigenfunction expansion method for the analysis of exponential decay curves. *J. Chem. Phys.* **64**:2772–2777 (1976).
18. Weiland, G. A., K. P. Minneman, and P. B. Molinoff. Fundamental difference between the molecular interactions of agonists and antagonists with the β-adrenergic receptor. *Nature* (*Lond.*) **281**:114–117 (1979).
19. Yeung, S. M. H., and R. D. Green. Agonist and antagonist affinities for inhibitory adenosine receptors are reciprocally affected by 5′-guanylylimidodiphosphate or *N*-ethylmaleimide. *J. Biol. Chem.* **258**:2334–2339 (1983).
20. Rodbell, M. The role of hormone receptors and GTP-regulatory proteins in membrane transduction. *Nature* (*Lond.*) **284**:17–22 (1980).
21. De Lean, A., B. F. Kilpatrick, and M. G. Caron. Dopamine receptor of the porcine anterior pituitary gland: evidence for two affinity states discriminated by both agonists and antagonists. *Mol. Pharmacol.* **22**:290–297 (1982).
22. Murphy, K. M. M., and S. H. Snyder. Heterogeneity of adenosine A_1 receptor binding in brain tissue. *Mol. Pharmacol.* **22**:250–257 (1982).
23. Kent, R. S., A. De Lean, and R. J. Lefkowitz. A quantitative analysis of *beta*-adrenergic receptor interactions: resolution of high and low affinity states of the receptor by computer modeling of ligand binding data. *Mol. Pharmacol.* **17**:14–23 (1980).
24. Weiland, G. A., K. P. Minneman, and P. B. Molinoff. Thermodynamics of agonist and antagonist interactions with mammalian β-adrenergic receptors. *Mol. Pharmacol.* **18**:341–347 (1980).
25. Zahniser, N. R., and P. B. Molinoff. Thermodynamic differences between agonist and antagonist interactions with binding sites for [^{3}H]spiroperidol in rat striatum. *Mol. Pharmacol.* **23**:303–309 (1983).
26. Barlow, R. B., N. J. M. Birdsall, and E. C. Hulme. Temperature coefficients of affinity constants for the binding of antagonists to muscarinic receptors in the rat cerebral cortex. *Br. J. Pharmacol.* **66**:587–590 (1979).
27. U'Prichard, D. C., and S. H. Snyder. Binding of ^{3}H-catcholamines to α-noradrenergic receptor sites in calf brain. *J. Biol. Chem.* **252**:6450–6463 (1977).
28. Simantov, R., A. M. Snowman, and S. H. Snyder. Temperature and ionic influences on opiate receptor binding. *Mol. Pharmacol.* **12**:977–986 (1976).
29. Molinoff, P. B., G. A. Weiland, K. A. Heidenreich, R. N. Pittman, and K. P. Minneman. Interactions of agonists and antagonists with β-adrenergic receptors. *Adv. Cyclic Nucleotide Res.* **14**:51–67 (1981).
30. De Lean, A., J. M. Stadel, and R. J. Lefkowitz. A ternary complex model explains the agonist-specific binding properties of the adenylate cyclase-coupled β-adrenergic receptor. *J. Biol. Chem.* **255**:7108–7117 (1980).

Send reprint requests to: Dr. Martin J. Lohse, Pharmakologisches Institut der Universität Heidelberg, 6900 Heidelberg, Federal Republic of Germany.